Journal of Photochemistry and Photobiology A: Chemistry 229 (2012) 1–10

Contents lists available at SciVerse ScienceDirect

Journal of Photochemistry and Photobiology A: Chemistry

journal homepage: www.elsevier.com/locate/jphotochem

# Photophysical study of the aggregation of naphthyl-, anthryl- and pyrenyl-adamantanebisurea derivatives

Vesna Blažek[a], Kata Mlinarić-Majerski[a], Wenwu Qin[b], Nikola Basarić[a,*]

[a] Department of Organic Chemistry and Biochemistry, Ruđer Bošković Institute, Bijenička cesta 54, 10000 Zagreb, Croatia
[b] Key Laboratory of Nonferrous Metal Chemistry and Resources Utilization of Gansu Province and State Key Laboratory of Applied Organic Chemistry, College of Chemistry and Chemical Engineering, Lanzhou University, Lanzhou 730000, PR China

ARTICLE INFO

*Article history:*
Received 14 September 2011
Received in revised form 6 December 2011
Accepted 10 December 2011
Available online 20 December 2011

*Keywords:*
Aggregation
Anthracenes
Fluorescence
Naphthalenes
Pyrenes
Ureas
Photophysics

ABSTRACT

Adamantaneurea derivatives **1**–**13** were synthesized and their photophysical properties investigated. The compounds **1**–**13** are comprised of a rigid adamantane moiety, 1 or 2 urea groups and different chromophores, as well as methylene spacer between the adamantane and the urea and/or between the urea and the chromophores. Fluorescence quantum yields and singlet excited state lifetimes were measured in $CH_3CN$ and DMSO. It was found that molecules with methylene spacer between the adamantane and the urea aggregate in $CH_3CN$, whereas aggregation was not observed in DMSO. The highest tendency to aggregation was observed for 9-aminoanthracene derivative **10** and pyrene derivative **13** which aggregate in both solvents. The aggregation probably takes place due to intermolecular H-bonds between the ureas and π,π-stacking of the aromatic chromophores. Pyrene **13** probably gives rise to excimers and intermolecular aggregates.



## 1. Introduction

Supramolecular self-assembly of molecules, since it was established by Lehn [1], turned to a widely accepted and powerful strategy to generate well-defined functional nanostructures and materials. For example, by use of tailored building blocks and noncovalent synthetic approach supramolecular gelators [2], liquid crystals [3], fibers [4], nanotubes [5], and vesicles [6] have been constructed. Another important aspect of self-assembly of molecules, is assembly of dyes [7], giving rise to J-aggregates [8] and H-aggregates [9]. The traditional classification of aggregates is based on the observed spectral shift of the absorption maximum compared to the one of the monomer. J-aggregates are characterized by a presence of an absorption band that is bathochromically shifted relative to the monomer absorption, and quite often, by higher fluorescence quantum yield [10]. On the other hand, H-aggregates exhibit hypsochromic shifts compared to the monomer absorption and their fluorescence is strongly quenched. Generally, for two parallely aligned dye molecules, two exciton states arise (that is, two absorption bands), one at the higher energy ("H-band") and one at the lower relative to the monomer band ("J-band"). Only when one of the exciton states is fully forbidden, spectra of perfect H- and J-aggregates occur, corresponding to the differences in packing and sign of the exciton coupling. The exciton state with parallel orientation of the transition dipoles to the lines joining centers of the individual molecules corresponds to J-aggregates (edge to edge arrangement), whereas H-aggregate consists of an one-dimensional array of molecules in which the transition moments of the individual monomers are aligned parallel to each other but perpendicular to the line joining their centers (face to face arrangement) [11].

Coordination chemistry of anions has in the past two decades developed into an important field of supramolecular chemistry because of the important role anions play in biological processes [12]. The Holy Grail of the anion supramolecular chemistry is finding receptors for the selective recognition of anionic species, particularly in the aqueous media, and transport through membranes [13]. Within the on-going research on supramolecular anion chemistry in our laboratory [14], we turned attention to adamantylurea derivatives [15]. Recently we reported on anion binding properties of adamantanebisurea derivatives **3**–**5** substituted with 2-naphthyl moiety [16]. The binding of $F^-$, $Cl^-$, $Br^-$, $OAc^-$, $HSO_4^-$, $NO_3^-$ and $H_2PO_4^-$, was investigated by UV–vis, fluorescence and NMR spectroscopy, and isothermal microcalorimetry. Measured association constants obtained by NMR and UV–vis spectroscopy differed significantly. The finding was explained by probable aggregation of the molecules in the concentration range for the NMR experiments, whereas aggregation probably did not take place in the diluted solutions for the UV–vis measurements [16]. It is well-known that urea derivatives aggregate and give rise

* Corresponding author. Tel.: +385 1 4561 141; fax: +385 1 4680 195.
*E-mail address:* nbasaric@irb.hr (N. Basarić).

1010-6030/$ – see front matter © 2011 Elsevier B.V. All rights reserved.
doi:10.1016/j.jphotochem.2011.12.005

to gels [17]. Moreover, Mendoza et al. recently reported on adamantanebisurea aggregation [18].

Herein we investigate photophysical properties of a series of adamantanebisurea derivatives **1**–**13**, with the aim of finding suitable receptors with desirable properties for the development of anion sensors. The compounds are strategically designed to probe for the possibility of aggregation, depending on the aromatic fluorophore, the presence of the methylene spacer between the rigid adamantane and the urea moieties, and between the urea moieties and the fluorophores. Contrary to the simple aliphatic bisurea derivatives [17], adamantyl moiety in **1**–**13** should hinder aggregation of the molecules, particularly in derivatives wherein ureas are directly connected to the adamantane. We performed a study by use of UV–vis spectroscopy, as well as steady state and time-resolved fluorescence.

## 2. Materials and methods

### 2.1. General

$^{1}H$ and $^{13}C$ NMR spectra were recorded on a Bruker Spectrometer at 300 or 600 MHz. All NMR spectra were measured in DMSO-$d_6$ using tetramethylsilane as a reference. High-resolution mass spectra (HRMS) were measured on an Applied Biosystems 4800 Plus MALDI TOF/TOF instrument. Melting points were obtained using an Original Kofler apparatus and are uncorrected. IR spectra were recorded on Perkin Elmer M-297 and ABB Bomem M-102 spectrophotometers. Solvents were purified by distillation. Adamantane diacids [19] were prepared in the laboratory according to known procedure. Amines and anthracene 9-carboxylic acid were obtained from the usual commercial sources.

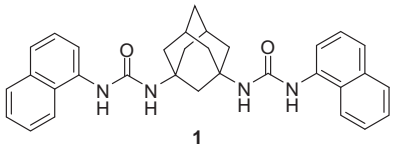


**1**

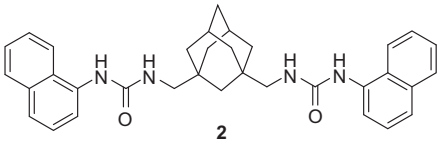


**2**

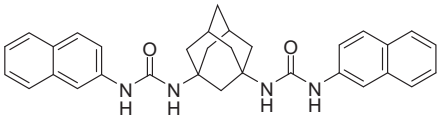


**3**

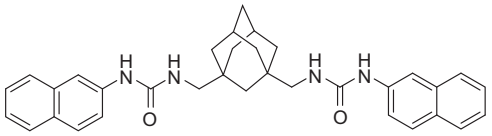


**4**

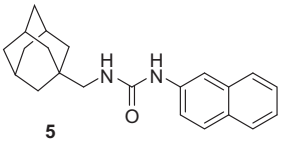


**5**

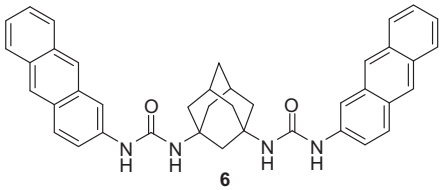


**6**

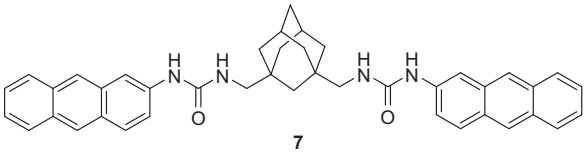


**7**

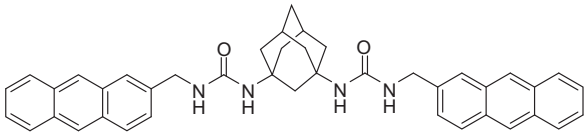


**8**

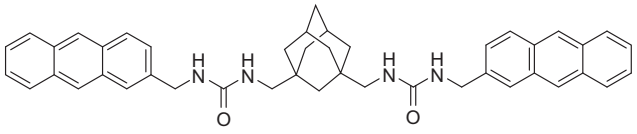


**9**

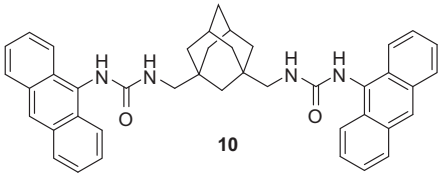


**10**

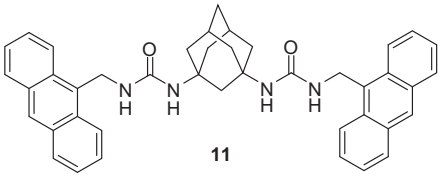


**11**

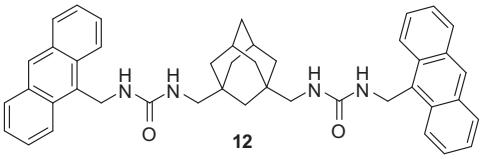


**12**

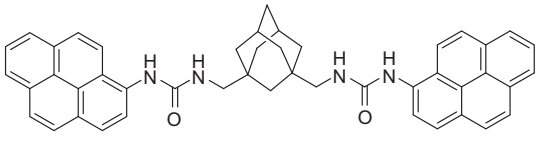


**13**

### 2.2. Synthesis of urea derivatives, general procedure

In a round bottom flask (50 mL), under a stream of $N_2$, the corresponding 1,3-adamantane dicarboxylic acid (200 mg, 0.89 mmol) was suspended in anhydrous toluene (10 mL) and triethylamine (TEA, 275 μL, 1.96 mmol) was added. The suspension was stirred at room temperature for 45 min, and then, diphenylphosphoryl azide (DPPA, 440 μL, 2.05 mmol) was added. The reaction mixture was heated at 40 °C for 1 h, and after that, 4 h at the temperature of the reflux. To this mixture a solution of amine (180 μL, 1.96 mmol) in 1 mL of dry toluene was added and the refluxing was continued for 16 h. The solvent was removed on the rotational evaporator and the residue was treated with methanol. The product in the crystal form was filtered off, washed with water and methanol, and dried in vacuum (100 mbar) at 60 °C for 1 h.

### 2.3. 1,3-Bis-[3-(naphthalen-1-yl)ureido]adamantane (**1**)

Following the general procedure **1** (170 mg, 38%) was obtained from 1,3-adamantane dicarboxylic acid (200 mg, 0.89 mmol), triethylamine (275 μL, 1.96 mmol), DPPA (440 μL, 2.05 mmol) and 1-aminonaphthalene (281 mg, 1.96 mmol), in 7 mL of dry toluene.

Colourless crystals, mp 233–234 °C; $^1$H NMR (DMSO-$d_6$, 600 MHz) $\delta$/ppm 8.36 (br s, 2H), 8.08 (d, 2H, $J$ = 8.6 Hz), 8.03 (dd, 2H, $J$ = 1.0 Hz, $J$ = 7.7 Hz), 7.88 (dd, 2H, $J$ = 1.2 Hz, $J$ = 8.0 Hz), 7.48–7.56 (m, 6H), 7.39 (t, 2H, $J$ = 8.0 Hz), 6.56 (br s, 2H), 2.32 (br s, 2H), 2.21 (br s, 2H), 1.99 (d, 4H, $J$ = 11.1 Hz), 1.93 (d, 4H, $J$ = 11.1 Hz), 1.60 (br s, 2H); $^{13}$C NMR (DMSO-$d_6$, 75 MHz) $\delta$/ppm 154.51 (s, 2C), 135.31 (s, 2C), 133.87 (s, 2C), 128.58 (d, 2C), 126.10 (d, 2C), 125.90 (d, 2C), 125.55 (d, 2C), 125.39 (s, 2C), 121.90 (d, 2C), 121.29 (d, 2C), 116.09 (d, 2C), 51.70 (t, 1C), 46.17 (s, 2C), 40.98 (t, 4C), 35.25 (t, 1C), 29.62 (d, 2C); IR (KBr) $\nu_{max}$/cm$^{-1}$ 1222 (m), 1258 (m), 1542 (s), 1645 (s), 2912 (m), 3335 (m); HRMS calcd for $C_{32}H_{32}N_4O_2$ + H 505.2598, found 505.2598.

### 2.4. 1,3-Bis-{[3-(naphthalen-1-yl)ureido]methyl} adamantane (**2**)

Following the general procedure **2** (290 mg, 69%) was obtained from 1,3-adamantane diacetic acid (200 mg, 0.79 mmol), triethylamine (245 μL, 1.74 mmol), DPPA (395 μL, 1.82 mmol) and 1-aminonaphthalene (250 mg, 1.74 mmol) in 7 mL of dry toluene.

Colourless crystals, mp 295–296 °C; $^1$H NMR (DMSO-$d_6$, 600 MHz) $\delta$/ppm 8.53 (br s, 2H), 8.11 (d, 2H, $J$ = 8.4 Hz), 8.07 (d, 2H, $J$ = 7.6 Hz), 7.88 (dd, 2H, $J$ = 7.7 Hz, $J$ = 1 Hz), 7.49–7.56 (m, 6H), 7.40 (t, 2H, $J$ = 7.7 Hz), 6.64 (t, 2H, $J$ = 5.9 Hz), 2.94 (d, 4H, $J$ = 5.9 Hz), 2.08 (br s, 2H), 1.61 (br s, 2H), 1.51 (d, 4H, $J$ = 11.7 Hz), 1.45 (d, 4H, $J$ = 11.7 Hz), 1.31 (br s, 2H); $^{13}$C NMR (DMSO-$d_6$, 150 MHz) $\delta$/ppm 155.71 (s, 2C), 135.30 (s, 2C), 133.69 (s, 2C), 128.38 (d, 2C), 125.94 (d, 2C), 125.68 (d, 2C), 125.32 (d, 2C), 125.07 (s, 2C), 121.60 (d, 2C), 121.14 (d, 2C), 115.69 (d, 2C), 50.73 (t, 2C), 42.55 (s, 2C), 39.39 (t, 4C), 36.08 (t, 1C), 34.09 (t, 1C), 27.85 (d, 2C), IR (KBr) $\nu_{max}$/cm$^{-1}$ 1238 (m), 1552 (s), 1624 (s), 2902 (m), 3330 (m); HRMS calcd for $C_{34}H_{36}N_4O_2$ + H 533.2911, found 533.2904.

### 2.5. 1,3-Bis-[3-(anthracene-2-yl)ureido]adamantane (**6**)

Following the general procedure **6** (226 mg, 84%) was obtained from 1,3-adamantane dicarboxylic acid (100 mg, 0.45 mmol), triethylamine (135 μL, 0.98 mmol), DPPA (220 μL, 1.03 mmol) and 2-aminoanthracene (190 mg, 0.98 mmol) in 10 mL of dry toluene.

Yellowish crystals; mp > 300 °C; $^1$H NMR (DMSO-$d_6$, 600 MHz) $\delta$/ppm 8.58 (s, 2H), 8.43 (s, 2H), 8.32 (s, 2H), 8.22 (s, 2H), 7.95–8.02 (m, 6H), 7.45 (dt, 2H, $J$ = 6.9 Hz, $J$ = 1.2 Hz) 7.41 (dt, 2H, $J$ = 6.9 Hz, $J$ = 1.2 Hz), 7.37 (dd, 2H, $J$ = 9.0 Hz, $J$ = 2.0 Hz), 6.18 (br s, 2H), 2.32 (br s, 2H), 2.22 (br s, 2H), 2.00 (d, 4H, $J$ = 10.9 Hz), 1.93 (d, 4H, $J$ = 10.9 Hz), 1.62 (br s, 2H); $^{13}$C NMR (DMSO-$d_6$, 150 MHz) $\delta$/ppm 154.14 (s, 2C), 137.56 (s, 2C), 132.28 (s, 2C), 131.76 (s, 2C), 129.84 (s, 2C), 128.73 (d, 2C), 128.09 (d, 2C), 127.92 (s, 2C), 127.54 (d, 2C), 125.77 (d, 2C), 125.48 (d, 2C), 124.41 (d, 2C), 123.97 (d, 2C), 120.91 (d, 2C), 110.50 (d, 2C), 51.56 (t, 1C), 45.94 (s, 2C), 40.81 (t, 4C), 35.12 (t, 1C), 29.48 (d, 2C); IR (KBr) $\nu_{max}$/cm$^{-1}$ 1222 (m), 1305 (m), 1547 (s), 1634 (s), 2912 (m), 3304 (m), 3386 (m); HRMS calcd for $C_{40}H_{36}N_4O_2$ + H 605.2911, found 605.2883.

### 2.6. 1,3-Bis-{[3-(anthracene-2-yl)ureido]methyl} adamantane (**7**)

Following the general procedure, **7** (145 mg, 65%) was obtained from 1,3-adamantane diacetic acid (89 mg, 0.35 mmol), triethylamine (110 μL, 0.79 mmol), DPPA (175 μL, 0.81 mmol) and 2-aminoanthracene (159 mg, 0.78 mmol) in 10 mL of dry toluene.

Grey crystals; mp 293–298 °C; $^1$H NMR (DMSO-$d_6$, 300 MHz) $\delta$/ppm: 8.69 (s, 2H), 8.42 (s, 2H), 8.32 (s, 2H), 8.19 (s, 2H), 7.94–8.04 (m, 6H), 7.38–7.48 (m, 6H), 6.30 (t, $J$ = 5.7 Hz 2H, H-7), 2.93 (d, 4H, $J$ = 5.7 Hz), 2.07 (br s, 2H), 1.60 (br s, 2H), 1.49 (d, 4H, $J$ = 11.7 Hz), 1.42 (d, 4H, $J$ = 11.7 Hz), 1.28 (br s, 2H); IR (KBr) $\nu_{max}$/cm$^{-1}$ 1240 (m), 1549 (s), 1650 (s), 2851 (w), 2905 (m), 3350 (m), HRMS calcd for $C_{42}H_{40}N_4O_2$ + Na 655.3043, found 655.3061.

### 2.7. 1,3-Bis-{[3-(anthracene-2-yl)methyl]ureido} adamantane (**8**)

Following the general procedure, **8** (35 mg, 28%) was obtained from 1,3-adamantane dicarboxylic acid (45 mg, 0.20 mmol), triethylamine (60 μL, 0.43 mmol), DPPA (98 μL, 0.45 mmol) and 2-aminomethylanthracene (90 mg, 0.43 mmol) in 10 mL of dry toluene.

Yellowish crystals; mp 280–282 °C; $^1$H NMR (DMSO-$d_6$, 300 MHz) $\delta$/ppm: 8.48–8.56 (m, 4H), 7.99–8.12 (m, 6H), 7.85 (br s, 2H), 7.36–7.57 (m, 6H), 6.25 (br s, 2H), 5.81 (br s, 2H), 4.36 (d, 4H, $J$ = 3.9 Hz), 2.06–2.20 (m, 4H), 1.75–1.95 (m, 8H), 1.52 (br s, 2H); IR (KBr) $\nu_{max}$/cm$^{-1}$ 1298 (m), 1559 (s), 1637 (s), 2860 (w), 2918 (m), 3305 (m), 3375 (m); HRMS calcd for $C_{42}H_{40}N_4O_2$ + K 671.2783, found 671.2781.

### 2.8. 1,3-Bis-({[3-(anthracene-2-yl)methyl]ureido}methyl)adamantane (**9**)

Following the general procedure, **9** (57 mg, 44%) was obtained from 1,3-adamantane diacetic acid (50 mg, 0.20 mmol), triethylamine (60 μL, 0.43 mmol), DPPA (98 μL, 0.45 mmol) and 2-aminomethylanthracene (90 mg, 0.43 mmol) in 10 mL of dry toluene.

Yellowish crystals; mp 292-297 °C; $^1$H NMR (DMSO-$d_6$, 300 MHz) $\delta$/ppm: 8.53 (br s, 2H), 8.48 (br s, 2H), 7.99–8.12 (m, 6H), 7.86 (br s, 2H), 7.39–7.54 (m, 6H), 6.41 (t, 2H, $J$ = 5.6 Hz), 5.98 (t, 2H, $J$ = 5.6 Hz), 4.42 (d, 4H, $J$ = 5.6 Hz), 2.83 (d, 2H, $J$ = 5.6 Hz), 2.01 (2H, br s), 1.54 (2H, br s), 1.42 (d, 4H, $J$ = 11.9 Hz), 1.33 (d, 4H, $J$ = 11.9 Hz), 1.12 (br s, 2H); IR (KBr) $\nu_{max}$/cm$^{-1}$ 1308 (m), 1559 (s), 1636 (s), 2853 (w), 2924 (m), 3430 (m); HRMS calcd for $C_{42}H_{40}N_4O_2$ + Na 683.3356, found 683.3339.

### 2.9. 1,3-Bis-{[3-(anthracene-9-yl)ureido]methyl} adamantane (**10**)

Following the general procedure, **10** (19 mg, 9%) was obtained from 1,3-adamantane diacetic acid (89 mg, 0.35 mmol), triethylamine (110 μL, 0.78 mmol), DPPA (175 μL, 0.81 mmol) and 9-aminoanthracene (150 mg, 0.78 mmol) in 10 mL of dry toluene.

*Alternative procedure*: In a two-neck round bottom flask, under a stream of $N_2$, 1,3-bis(aminomethyl)adamantane dihydrochloride

(259 mg, 0.97 mmol) was suspended in 75 mL of anhydrous THF, and by use of a syringe triethylamine (410 μL, 2.91 mmol) was added. By use of a dropping funnel, a solution of 9-anthraceneisocyanate (425 mg, 1.94 mmol) in 30 mL anhydrous THF was added over 30 min. The reaction mixture was stirred at room temperature for 1 h and heated at reflux over night. The cooled reaction mixture was filtered through a sinter funnel to separate the precipitated product. The product was washed by THF, water and methanol, and dried in vacuum (100 bar) at 60 °C for 1 h to yield 420 mg (69%) of the pure product.

Yellowish crystals; mp > 320 °C; $^1$H NMR (DMSO-$d_6$, 300 MHz) $\delta$/ppm 8.52 (br s, 2H), 8.49 (br s, 2H), 8.04–8.20 (m, 8H), 7.46–7.58 (m, 8H), 6.38 (br s, 2H), 2.93 (d, 4H, $J$ = 5.5 Hz), 2.10 (br s, 2H), 1.64 (br s, 2H), 1.54 (d, 4H, $J$ = 12.2 Hz), 1.44 (d, 4H, $J$ = 12.2 Hz), 1.32 (br s, 2H); $^{13}$C NMR (DMSO-$d_6$, 75 MHz) $\delta$/ppm 157.26 (s, 2C), 131.42 (s, 2C), 130.68 (s, 2C), 128.66 (s, 2C), 128.28 (d, 2C), 125.54 (d, 2C), 125.37 (d, 2C), 124.77 (d, 2C), 124.08 (d, 2C), 51.00 (t, 2C), 42.83 (s, 2C), 36.18 (t, 1C), 34.42 (t, 1C), 27.96 (d, 2C), C-3 is covered with the signal of DMSO-$d_6$; IR (KBr) $\nu_{max}$/cm$^{-1}$ 1238 (m), 1552 (s), 1619 (s), 2902 (m), 3257 (m), 3319 (m); HRMS calcd for $C_{42}H_{40}N_4O_2$ + H 633.3224, found 633.3207.

### 2.10. 1,3-Bis-{[3-(anthracene-9-yl)methyl]ureido} adamantane (**11**)

Following the general procedure, **11** (71 mg, 79%) was obtained from 1,3-adamantane dicarboxylic acid (100 mg, 0.45 mmol), triethylamine (135 μL, 0.98 mmol), DPPA (220 μL, 1.03 mmol) and 9-aminomethylanthracene (213 mg, 0.98 mmol) in 10 mL of dry toluene.

Yellowish crystals; mp > 320 °C; $^1$H NMR (DMSO-$d_6$, 600 MHz) $\delta$/ppm 8.59 (s, 2H), 8.41 (d, 2H, $J$ = 8.8 Hz), 8.11 (d, 2H, $J$ = 8.3 Hz), 7.59 (dd(t), 4H, $J$ = 7.2 Hz), 7.53 (dd(t), 4H, $J$ = 7.4 Hz), 6.10 (t, 2H, $J$ = 5.3 Hz), 5.53 (br s, 2H), 5.15 (d, 4H, $J$ = 5.3 Hz), 2.08 (br s, 2H), 1.99 (br s, 2H), 1.78 (br s, 8H), 1.49 (br s, 2H); IR (KBr) $\nu_{max}$/cm$^{-1}$ 1225 (w), 1292 (w), 1338 (w), 1357 (w), 1560 (s), 1623 (s), 2910 (m), 3345 (m); HRMS calcd for $C_{42}H_{40}N_4O_2$ + Na 655.3043, found 655.3061.

### 2.11. 1,3-Bis-({[3-(anthracene-9-yl)methyl]ureido}methyl)adamantane (**12**)

Following the general procedure, **12** (75 mg, 52%) was obtained from 1,3-adamantane diacetic acid (55 mg, 0.22 mmol), triethylamine (67 μL, 0.49 mmol), DPPA (109 μL, 0.50 mmol) and 9-aminomethylanthracene (100 mg, 0.48 mmol) in 10 mL of dry toluene.

Yellowish crystals; mp > 320 °C; $^1$H NMR (DMSO-$d_6$, 600 MHz) $\delta$/ppm: 8.59 (s, 2H), 8.42 (d, 2H, $J$ = 8.5 Hz), 8.11 (d, 2H, $J$ = 8.1 Hz), 7.51–7.58 (m, 8H), 6.22 (t, 2H, $J$ = 5.1 Hz), 5.64 (t, 2H, $J$ = 5.7 Hz), 5.20 (d, 4H, $J$ = 5.1 Hz), 2.74 (d, 4H, $J$ = 5.7 Hz), 1.93 (br s, 2H), 1.46 (br s, 2H), 1.32 (d, 4H, $J$ = 11.6 Hz), 1.22 (d, 4H, $J$ = 11.6 Hz), 1.04 (br s, 2H); IR (KBr) $\nu_{max}$/cm$^{-1}$ 1244 (m), 1559 (s), 1604 (s), 2847 (w), 2905 (m), 3324 (m); HRMS calcd for $C_{44}H_{44}N_4O_2$ + Na 683.3356, found 683.337.

### 2.12. 1,3-Bis-{[3-(pyrene-1-yl)ureido]methyl}adamantane (**13**)

Following the general procedure, **13** (158 mg, 58%) was obtained from 1,3-adamantane diacetic acid (100 mg, 0.40 mmol), triethylamine (122 μL, 0.87 mmol), DPPA (196 μL, 0.91 mmol) and 1-aminopyrene (189 mg, 0.87 mmol) in 10 mL of dry toluene.

Grey crystals; mp 299–302 °C; $^1$H NMR (DMSO-$d_6$, 600 MHz) $\delta$/ppm: 8.96 (br s, 2H), 8.71 (d, 2H, $J$ = 8.3 Hz), 8.32 (d, 2H, $J$ = 9.3 Hz), 8.14–8.23 (m, 8H), 7.98–8.07 (m, 6H), 6.75 (t, 2H, $J$ = 5.7 Hz), 3.02 (d, 4H, $J$ = 5.7 Hz), 2.13 (br s, 2H), 1.66 (br s, 2H), 1.57 (d, 4H, $J$ = 11.6 Hz), 1.52 (d, 4H, $J$ = 11.6 Hz), 1.40 (br s, 2H); IR (KBr) $\nu_{max}$/cm$^{-1}$ 1239 (m), 1559 (s), 1623 (s), 2899 (m), 3337 (m); HRMS calcd for $C_{46}H_{40}N_4O_2$ + Na 703.3043, found 703.3066.

### 2.13. UV–vis measurements

The UV–vis measurements were performed on a Varian Carry 100 spectrometer. The compounds were dissolved in $CH_3CN$ (J.T. Baker or Caledon, HPLC grade), or DMSO (Sigma–Aldrich or Fluka, UV-spectroscopy grade). The measurements were performed at 20 °C.

### 2.14. Steady state and time-resolved fluorescence measurements

The steady state measurements were performed on a Photon Technology International (PTI) Quanta-Master QM-2 luminescence spectrometer or Cary Eclipse Varian spectrometer. The compounds were dissolved in $CH_3CN$ (HPLC grade), or DMSO (UV-spectroscopy grade) and the concentrations were adjusted to have absorbance at the excitation wavelength < 0.1. Solutions were purged with nitrogen for 30 min prior to analysis. The measurements were performed at 20 °C. Fluorescence quantum yields were determined by comparison of the integral of the emission bands with the one of NATA (N-acetyltryptophanamide)/$H_2O$ ($\Phi$ = 0.14) or quinine sulfate/0.5 M $H_2SO_4$ ($\Phi$ = 0.54) [20]. Typically, three absorption traces were recorded (and averaged) and five fluorescence emission traces, excited at five different wavelengths. Five quantum yields were calculated and the mean value reported.

Fluorescence decay histograms were obtained on an Edinburgh instrument OB920, equipped with a hydrogen flash lamp or light emitting diode (excitation wavelength 280, 310, or 365 nm), using time-correlated single photon counting technique in 1023 channels. Histograms of the instrument response functions (using LUDOX scatterer), and sample decays were recorded until they typically reached $3 \times 10^3$ counts in the peak channel. The half width of the instrument response function was typically ~1.5 ns. The time increment per channel was 0.019, 0.049, 0.098 or 0.19 ns. Obtained histograms were fitted as sums of exponential using Gaussian-weighted non-linear least-squares fitting based on Marquardt–Levenberg minimization implemented in the software package of the instrument. The fitting parameters (decay times and pre-exponential factors) were determined by minimizing the reduced chi-square $\chi^2$. Additional graphical method was used to judge the quality of the fit that included plots of surfaces ("carpets") of the weighted residuals vs. channel number.

## 3. Results and discussion

### 3.1. Synthesis

Urea derivatives **1**–**13** were prepared in moderate to good yields according to a modification of the published procedure from the corresponding carboxylic acids that were transformed to isocyanates in situ and reacted with amines (Eq. (1)) [18]. The exception was compound **10** which was prepared also in a procedure from adamantanediamine derivative and anthracene isocyanate (Eq. (2)). The alternative procedure furnished product **10** of higher purity. Prior to fluorescence measurements, compounds were purified three times by crystallization from DMF.

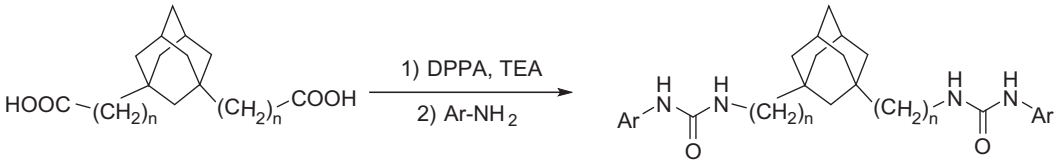


(1)

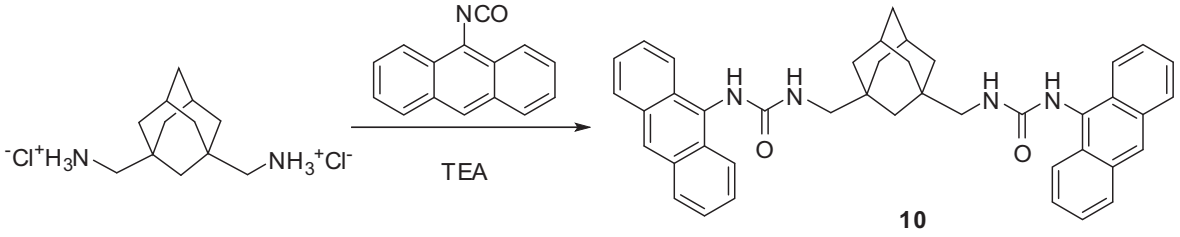


(2)

### 3.2. UV–vis and fluorescence measurements

Due to low solubility of **1**–**13** in most solvents, measurements could only be performed in $CH_3CN$ and DMSO. For example, solubility of **6**–**13** in $CH_3CN$ is lower than $5 \times 10^{-6}$ mol/dm$^3$, being somewhat higher in DMSO (reaching $10^{-3}$ mol/dm$^3$). The maxima in the absorption spectra and the corresponding molar absorption coefficients, and maxima in the fluorescence spectra are compiled in Table 1. Quantum yields of fluorescence were measured by use of two reference compounds, NATA and quinine sulfate. The lifetimes were measured by single-photon timing method. The results are compiled in Table 2.

Absorption spectra of **1**–**13** are generally characterized by the expected absorption bands corresponding to the chromophores in 1-amino (~310 nm) or 2-aminonaphthalene (~340 nm), 2-aminoanthracene (300–420 nm), 2-methylanthracene (300–400 nm), 9-aminoanthracene (350–420 nm), 9-methylanthracene (320–400 nm) and 1-aminopyrene (320–400 nm) [21]. However, comparison of the normalized absorption spectra in $CH_3CN$ and DMSO, or spectra of different compounds having the same chromophore reveal differences in the absorption properties, due to the formation of aggregates (vide infra) which are also indicated in the corresponding fluorescence spectra.

1-Naphthyl derivatives, compounds **1** and **2**, have the same chromophore. Consequently, they should exhibit the same or similar spectral properties. Indeed, normalized absorption spectra in DMSO perfectly overlap, as well as fluorescence spectra recorded in DMSO. However, the absorption spectra of **1** and **2** in $CH_3CN$ show slight difference which becomes more pronounced in the corresponding fluorescence spectra (Fig. 1). Compound **2** exhibit bathochromic shift in the absorption spectrum of 5 nm, whereas the difference of 20 nm was observed in the fluorescence spectra. In addition to bathochromic shifts in the spectra, quantum yield of fluorescence slightly decreased from 0.39 to 0.32. The finding suggests aggregation of **2** in $CH_3CN$, which however does not take place in DMSO. Interestingly, after heating of the $CH_3CN$ solution of **2** and cooling to the room temperature, normalized fluorescence spectra of **1** and **2** showed perfect overlap indicating that aggregates were not present anymore. Aggregation is probably a slow process taking place over several hours, as reported for some other urea derivatives [17]. Thus, immediately after the heating and cooling, aggregates were not present in the solution. Fluorescence decay for both compounds in both solvents revealed bi-exponential behavior. Bi-exponential decay of 1-aminonaphthalenes has been reported [22]. It may be attributed to the population of a CT state in a polar solvent [22], presence of $L_a$ and $L_b$ excited states of the 1-aminonaphthalene chromophore [23], or the presence of rotamers (due to restricted rotation around the naphthalene nitrogen or the nitrogen carbonyl bond) with different singlet excited state lifetimes. Similar to the steady-state spectra, fluorescence decay of **2** in $CH_3CN$ changed after heating and cooling of the solution (Table 2), in agreement with the disappearance of the aggregates after heating.

Urea derivatives **1**–**13** can in principle aggregate due to the formation of intermolecular H-bonds between the urea moieties [17], and π,π-stacking of the aromatic rings [24]. Observation of the aggregation of derivative **2** wherein the ureas are separated from the rigid bulky adamantanes, in $CH_3CN$ and not in DMSO, suggests that molecules aggregate due to intermolecular H-bonds between the urea moieties which is not possible in **1** due to the sterical hindrance of the adamantane. However, since we observed only small changes in the absorption spectra for the 1-naphthyl derivative we cannot undoubtedly assign the aggregates to H- or J-type. Non-observation of the aggregation in DMSO is in line with DMSO participating in H-bonding with the urea and preventing the aggregation.

Contrary to 1-naphthalenes, 2-naphthyl derivatives **3**–**5** do not aggregate, at least not in the concentration range for the UV–vis and fluorescence measurements ($c = 10^{-6}$ to $10^{-4}$ mol dm$^{-3}$). That is demonstrated by perfect spectral overlap of their absorption spectra, as well as their fluorescence spectra in both solvents (see the Supporting Information). In addition, fluorescence decays are characterized by single-exponential functions revealing lifetimes of the corresponding $S_1$ states. However, in higher concentrations typical for the NMR experiments ($c = 10^{-3}$ to $10^{-2}$ mol dm$^{-3}$), aggregation of **3**–**5** was observed [16]. It is also interesting to note that lifetimes in DMSO are somewhat shorter than in $CH_3CN$. The finding is logical since DMSO forms complexes with the urea moiety. Probably, due to the H-bonding between DMSO and the urea NH, delocalization of the lone pair of the NH increases over the naphthalene moiety in the excited state, and this enhances intersystem crossing, as well as internal conversion.

Since we observed different photophysical behavior of 1- and 2-naphthyl derivatives, which we associated with the aggregation of **2**, we attempted to measure time-resolved fluorescence anisotropy where increase in diffusion correlation time would clearly point to the presence of larger molecular aggregates. Compounds **1**–**4** were not soluble in glycerol, so we tried to measure the anisotropy decay in DMSO at 15 °C near the freezing of DMSO. However, the measurements by use of parallely or perpendicularly oriented polarizers showed no difference, so the anisotropy decay could not be measured. Although the molecules near the freezing point are probably not very mobile and show slow rotational diffusion, segmental rotations around single bonds in the molecule are still probably possible, resulting in a fast decay of the anisotropy, faster than the time resolution of the nanosecond set-up.

**Table 1**
Maxima in the absorption and emission spectra for **1**–**13** in $CH_3CN$ and DMSO.

| Compound | $CH_3CN$ | | | DMSO | | |
|---|---|---|---|---|---|---|
| | $\lambda_{abs}$/nm | $\varepsilon$/dm$^3$ mol$^{-1}$ cm$^{-1}$ | $\lambda_{em}$/nm | $\lambda_{abs}$/nm | $\varepsilon$/dm$^3$ mol$^{-1}$ cm$^{-1}$ | $\lambda_{em}$/nm |
| **1** | 219, 299, 326 | 15,600 ± 500 (301 nm) | 377 | 312, 327 | 15,700 ± 500 (315 nm) | 380 |
| **2** | 219, 304, 326 | 15,000 ± 300 (301 nm) | 398 | 310, 327 | 30,300 ± 400 (310 nm) | 380 |
| **3** | 213, 247, 271, 281, 292, 324, 336 | 19,000 ± 1000 (281 nm) | 365 | 258, 273, 284, 295, 327, 340 | 22,000 ± 2000 (284 nm) | 370 |
| **4** | 213, 247, 271, 281, 292, 324, 336 | 18,000 ± 5000 (281 nm) | 365 | 259, 273, 284, 294, 328, 340 | 22000 ± 2000 (284 nm) | 370 |
| **5** | 213, 247, 271, 281, 292, 324, 336 | 10,000 ± 1000 (280 nm) | 365 | 257, 273, 284, 294, 328, 339 | 9900 ± 600 (284 nm) | – |
| **6** | 263, 272, 321, 336, 355, 380, 398 | – | 442 | 274, 322, 339, 357, 387, 407 | 7200 ± 100 (357 nm) | 453 |
| **7** | 262, 320, 336, 354, 379, 396 | – | 441, 478 | 271, 322, 338, 357, 387, 407 | 7200 ± 300 (357 nm) | 453 |
| **8** | 254, 276, 325, 339, 356, 376 | – | 384, 408, 430 | 257, 282 328, 342, 360, 380, 407 | - | 390, 413, 435 |
| **9** | 254, 269, 277, 324, 340, 357, 376 | – | 407, 426 | 258, 282 328, 344, 361, 380 | 10,400 ± 600 (361 nm) | 390, 413, 433 |
| **10** | 252, 368, 386, 412 | – | 474 | 260, 352, 369, 388 | 14,400 ± 300 (372 nm) | 450 |
| **11** | – | – | – | 260, 334, 350, 368, 390 | 17,000 ± 1000 (368 nm) | 393, 417, 442, 470 |
| **12** | – | – | – | 260, 335, 350, 369, 390 | 14,600 ± 500 (368 nm) | 393, 417, 442, 470 |
| **13** | 243, 282, 346, 389 | | 395, 416, 506 | 286, 356, 371, 391 | 37,000 ± 1000 (356 nm) | 403, 418 |

Anthracene derivatives can be classified in four groups, having 2-amino, 2-methyl, 9-amino or 9-methyl substitution. Similarly to 1-naphthyl derivatives **1** and **2**, 2-anthryl derivatives **6** and **7** exhibit spectral differences in $CH_3CN$, but not in DMSO (Fig. 2 and Supporting Information). Namely, for these two compounds, normalized absorption and fluorescence spectra in DMSO exhibit almost perfect overlap, which is in accordance with the existence of the same chromophore in these molecules. However, in $CH_3CN$, the absorption spectrum of **7**, compared to **6**, shows a shoulder at longer wavelengths (420–500 nm) and an increased absorption band at 320 nm. The observed low-energy shoulder in the absorption spectrum of **7** could in principle correspond to light scattering, due to formation of nano- or microcrystals. However, excitation spectra of **7** recorded at different emission wavelengths

**Table 2**
Photophysical properties of **1**–**13** in $CH_3CN$ and DMSO.

| Compound | DMSO | | $CH_3CN$ | |
|---|---|---|---|---|
| | $\Phi$ | $\tau$/ns (%) | $\Phi$ | $\tau$/ns (%) |
| **1** | – | 6.57 ± 0.03 (91)<br>3.20 ± 0.02 (9) | 0.394 ± 0.004[a] | 7.2 ± 0.1 (96)<br>1.4 ± 0.1 (4) |
| **2** | – | 4.9 ± 0.1 (40)<br>8.2 ± 0.1 (60) | 0.32 ± 0.04[a,d] | 6 ± 1 (40)[c]<br>20 ± 5 (60)[c]<br>6.4 ± 0.1 (74)[d]<br>2.3 ± 0.1 (26)[d] |
| **3** | – | 6.30 ± 0.02 | 0.192 ± 0.006[b] | 7.3 ± 0.1 |
| **4** | – | 6.65 ± 0.05 | 0.198 ± 0.005[b] | 7.9 ± 0.1 |
| **5** | – | 6.56 ± 0.01 | 0.12 ± 0.02[b] | 7.5 ± 0.1 |
| **6** | 0.68 ± 0.08[a] | 19.5 ± 0.2 | 0.52 ± 0.03[a] | 22.5 ± 0.1 |
| **7** | 0.68 ± 0.08[a] | 17.5 ± 0.2 | 0.15 ± 0.02[a] | 0.2 ± 0.1 (20%)<br>6 ± 1 (25%)<br>18 ± 2 (55%) |
| **8** | 0.112 ± 0.003[a] | 1.7 ± 0.2 (15%)<br>3.7 ± 0.1 (85%) | 0.073 ± 0.006[a] | 0.4 ± 0.1 (10%)<br>3.0 ± 0.1 (25%)<br>18 ± 1 (65%) |
| **9** | 0.083 ± 0.004[a] | 1.1 ± 0.1 (20%)<br>3.3 ± 0.1 (70%)<br>11 ± 1 (10%) | 0.076 ± 0.003[a] | 1.1 ± 0.1 (10%)<br>3 ± 1 (35%)<br>18 ± 1 (55%) |
| **10** | 0.102 ± 0.009[a] | 1.4 ± 0.1 (65%)<br>2.3 ± 0.1 (35%) | 0.0132 ± 0.0002[a] | 0.60 ± 0.01 (85%)<br>2.6 ± 0.1 (15%) |
| **11** | 0.4 ± 0.1[a] | 1.0 ± 0.4 (2%)<br>7.6 ± 0.1 (98%) | –[e] | –[e] |
| **12** | 0.4 ± 0.1[a] | 1.5 ± 0.1 (2%)<br>7.4 ± 0.1 (98%) | –[e] | –[e] |
| **13** | 0.50 ± 0.03[a] | 0.9 ± 0.1 (2%)<br>4.1 ± 0.2 (95%)<br>40 ± 5 (3%) | 0.18 ± 0.03[a] | 0.8 ± 0.2 (20%)<br>4.0 ± 0.2 (50%)<br>25 ± 5 (30%) |

[a] Determined by using quinine sulfate as a reference compound ($\Phi$ = 0.54) [20].
[b] Determined by use of NATA as a reference compound ($\Phi$ = 0.14) [20].
[c] Sample not heated.
[d] Sample heated and cooled to room temperature.
[e] Sample not soluble in $CH_3CN$.

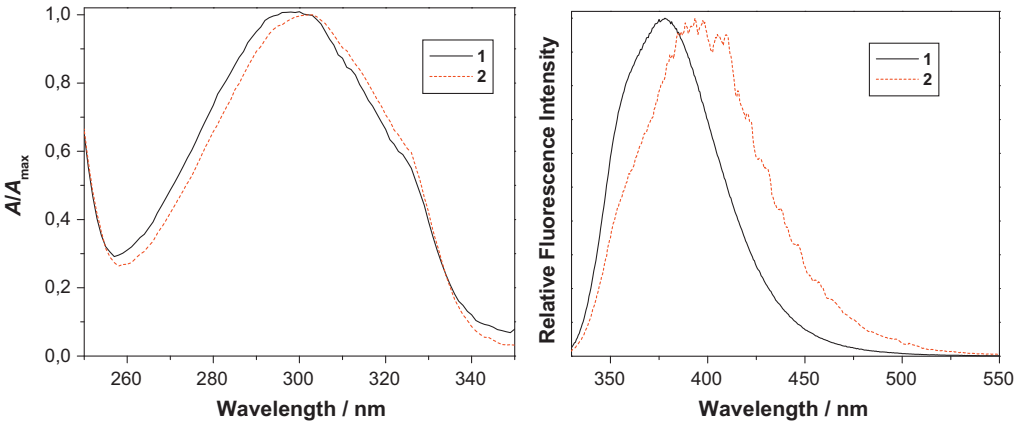


**Fig. 1.** Absorption spectra (left) and fluorescence spectra (right, $\lambda_{ex}$ = 310 nm) of **1** and **2** in $CH_3CN$.

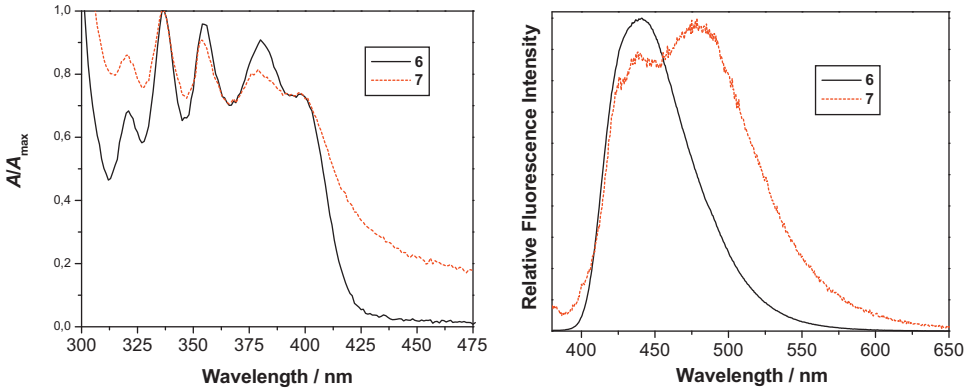


**Fig. 2.** Absorption spectra (left) and fluorescence spectra (right, $\lambda_{ex}$ = 310 nm) of **6** and **7** in $CH_3CN$.

clearly indicate a presence of different emitting species depending on the observation emission wavelengths (see the Supporting Information). Moreover, in the fluorescence spectrum of **7** in $CH_3CN$, besides an emission band at 440 nm, one additional band appears at 480 nm. In addition to the changes in the emission spectrum, fluorescence quantum yield of **7** in $CH_3CN$ is four times lower than for **6**, whereas they are the same in DMSO solutions ($\Phi$ = 0.68, the reported values of fluorescence quantum yield and lifetime for 2-aminoanthracene in polar solvent is $\Phi$ = 0.57 and $\tau$ = 30.8 ns) [20]. Decay of the fluorescence is single-exponential for **6** in both solvents, as well as for **7** in DMSO. However, for **7** in $CH_3CN$ the decay becomes three-exponential (Fig. 3). All these findings are consistent with formation of aggregates of **7** in $CH_3CN$ solution, whereas in DMSO aggregation probably does not take place. Most probably, DMSO engages in hydrogen bonding with the urea moieties and thus breaks the intermolecular H-bonds between the ureas which cause the aggregation. Furthermore, the observation that **7** aggregates (and **6** probably does not) only in $CH_3CN$, in addition to the observed spectral changes, suggest that aggregates are probably formed due to both intermolecular H-bonds between the urea moieties and the π,π-stacking. Although the absorption spectral changes are not indicative neither for J- nor H-aggregates, quenched fluorescence of **7** in $CH_3CN$ (compared to DMSO solution or fluorescence of **6** in $CH_3CN$) suggests formation of H-aggregates. However, with the present data no unambiguous conclusion regarding the type of the aggregates can be made. In addition, although we have not observed spectral changes that would suggest aggregation of **6**, it may be possible, but molecules do not approach one another sufficiently to get the spectral changes.

2-Methylanthracene derivatives **8** and **9** are characterized by absorption spectra that in $CH_3CN$ exhibit additional hypsochromic bands (Fig. 4 and the Supporting Information) compared to DMSO solution, suggesting formation of H-aggregates. In addition, in the absorption spectrum of **8** in $CH_3CN$, a shoulder appears at longer wavelengths (400–420 nm) suggesting that several types of aggregates may be formed, those with the parallel and antiparallel

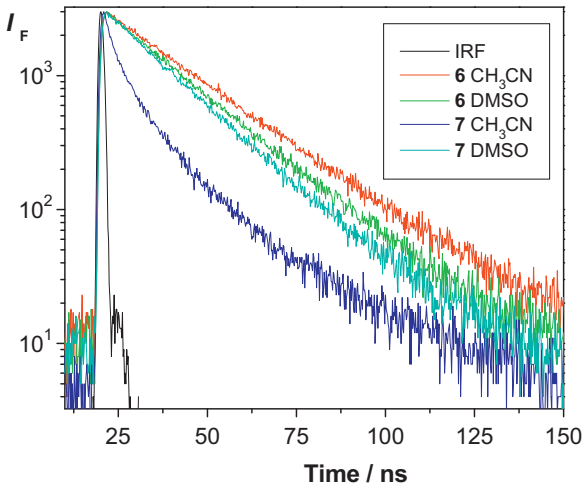


**Fig. 3.** Fluorescence decay of **6** and **7** in $CH_3CN$ and DMSO measured by single-photon timing ($\lambda_{ex}$ = 365 nm, $\lambda_{em}$ = 450 nm).

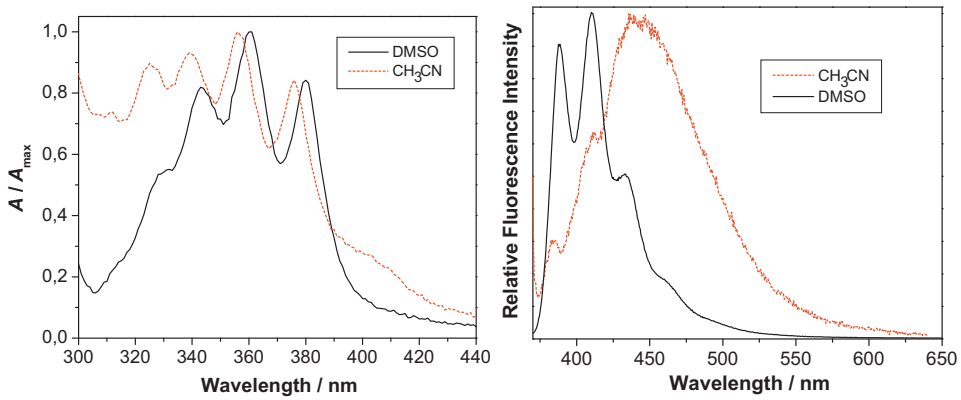


**Fig. 4.** Absorption spectra (left) and fluorescence spectra (right, $\lambda_{ex}$ = 365 nm) of **8** in $CH_3CN$ and DMSO.

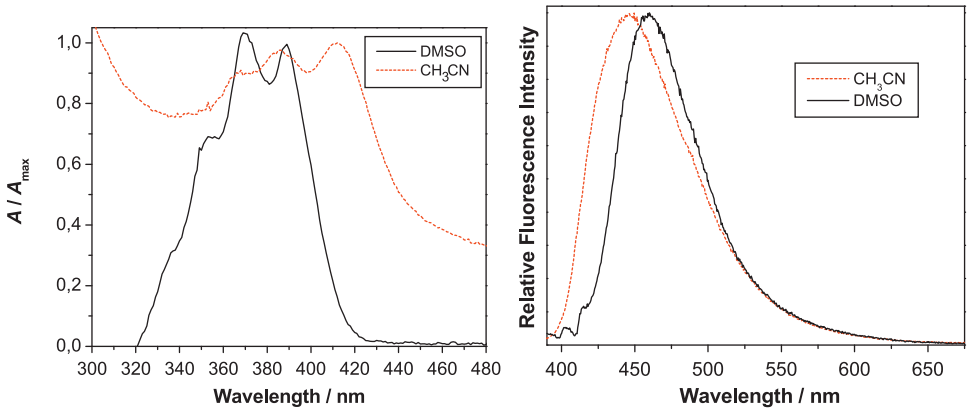


**Fig. 5.** Absorption spectra (left) and fluorescence spectra (right, $\lambda_{ex}$ = 365 nm) of **10** in $CH_3CN$ and DMSO.

orientation of the transition moments. Fluorescence spectra of **8** and **9** in DMSO are characterized by a typical structured anthracene emission band at 375–500 nm with the characteristic vibronic progression, whereas fluorescence spectra in $CH_3CN$ have no vibronic structure and are significantly bathochromically shifted compared to those in DMSO (100 nm) (Fig. 4). Fluorescence quantum yields for **8** and **9** in both solvents are six to seven times lower compared to the quantum yields of 2-aminoanthracenes **6** and **7**, and the decay of the fluorescence cannot be described by single exponential functions. Fluorescence decays for **8** and **9** in DMSO are characterized by the presence of a major decay component with 3–4 ns, typical for 2-methylanthracenes [25]. The shorter decay times observed in DMSO may be associated to the presence of rotamers with different $S_1$ lifetimes. However, long decay times (18 ns) observed in $CH_3CN$, together with the fluorescence spectral characteristics strongly indicate formation of aggregates in that solvent.

9-Anthryl derivative **10** is very weakly soluble in $CH_3CN$, whereas **11** and **12** are completely insoluble. Therefore, 9-anthrylmethyl derivatives were measured only in DMSO. The photophysical properties of **11** and **12** in DMSO do not deviate from the expected behavior of the methylanthracene chromophore. Their absorption spectra have a band in 350–400 nm region with the characteristic structured pattern. The emission spectra have maxima in 375–450 nm and the spectra forming the perfect mirror image to the absorption. Fluorescence quantum yields and singlet excited state lifetimes are comparable to the reported for 9-methylanthracenes in polar solvent ($\Phi$ = 0.33, $\tau$ = 5.8 ns) [20]. Consequently, these derivatives probably do not form aggregates in DMSO, or if they do, molecules pack in a way not to induce spectral changes. On the contrary, aminoanthracene derivative **10** exhibited quite different photophysical properties (Fig. 5). The absorption spectrum in $CH_3CN$ clearly indicates additional bands at shorter and longer wavelengths than observed in DMSO. The finding may be explained by formation of aggregates, and formation of microcrystals which cause light scattering. The excitation spectra in both solvents show perfect overlap, regardless of the observation emission wavelength, indicating that only one type of the species contribute to the observed emission. The emission in $CH_3CN$ is ten times lower than in DMSO. However, measured lifetimes in both solvents are similar. These findings indicate that in $CH_3CN$ solution only non-aggregated molecules fluoresce, whereas aggregates are not emissive.

Pyrene derivatives are generally known for their tendency to form aggregates characterized by characteristic long-wavelength fluorescence [26] and multi-exponential decays [27]. Similarly to

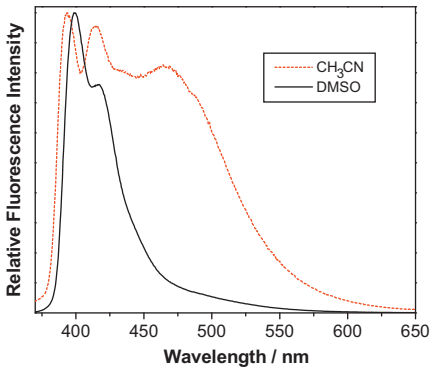


**Fig. 6.** Fluorescence spectra of **13** in $CH_3CN$ and DMSO ($\lambda_{ex}$ = 365 nm).

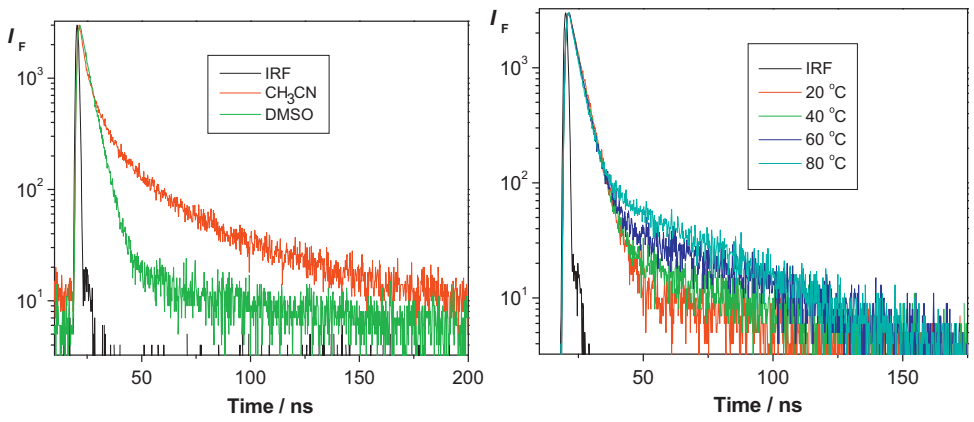


**Fig. 7.** Fluorescence decay of **13** in $CH_3CN$ and DMSO (left) and in DMSO at different temperatures (right) ($\lambda_{ex}$ = 365 nm, $\lambda_{em}$ = 440 nm).

above findings, derivative **13** exhibited different photophysical behavior in $CH_3CN$ and DMSO. In the absorption spectrum of **13** in $CH_3CN$, compared to DMSO, additional broad bands at longer and shorter wavelength can be seen (see the Supporting Information). Similarly to the spectra of **10**, the finding suggests formation of aggregates, or microcrystals which cause light scattering. However, the excitation spectra measured in $CH_3CN$ at different emission wavelength (390–520 nm, see the Supporting Information) do not overlap, indicating that different species contribute to the emission. Almost perfect overlap is observed for the excitation spectra taken in DMSO. In the emission spectra in DMSO the maxima are observed at 400 and 420 nm, with only a weak shoulder at ~475 nm. On the contrary, in $CH_3CN$, besides bands at 400 and 420 nm, a strong structureless band at 475 nm dominates the spectrum (Fig. 6) corresponding to the emission from the aggregated pyrene moieties. All the above findings are in agreement with the aggregation of pyrene moieties in $CH_3CN$.

Does **13** form intramolecular or intermolecular aggregates? Steady-state fluorescence spectra of **13** in $CH_3CN$ were recorded at different concentrations (corresponding to $A_{365}$ = 0.01–0.1, $c \sim 3 \times 10^{-7}$ to $3 \times 10^{-6}$ mol dm$^{-3}$; solubility limit for **13** in $CH_3CN$ is $\sim 3 \times 10^{-6}$ mol dm$^{-3}$). However, neither spectral shape nor the quantum yield of the fluorescence changed on dilution of the solution. The finding suggests that aggregation is not due to the intermolecular, but rather intramolecular interaction of the two arms bearing urea and pyrene. Furthermore, the intramolecular interaction of the pyrenes may be formed in the ground state, or in the excited state (that is, molecule may form intramolecular excimers). It should be mentioned that the intramolecular aggregation of the chromophores should be principally possible in all derivatives bearing methylene spacers between the ureas and the adamantane. However, except for **13** wherein there is the biggest π-surface for the π,π-stacking, it is unlikely that the molecules adopt conformation wherein the intramolecular aggregation would occur. The dilution experiment for **13** suggests that the observed phenomena in the spectra are due to an intramolecular process, or that intermolecular aggregates are formed in $CH_3CN$ already at very low concentrations ($c = 3 \times 10^{-7}$ mol dm$^{-3}$), so that change of the concentration in the investigated range did not influence relative ratio of the aggregated and non-aggregated molecules.

SPT measurements for **13** in both solvents gave rise to decays that could be best fitted with three-exponential functions. The multi-exponential decay of fluorescence suggests that aggregates (or excimers) are formed in both solvents (Fig. 7 and Table 3). However, in DMSO, the multiexponential decay may be due to a presence different rotamers. To probe for the aggregation in DMSO fluorescence decays were measured at different temperatures (Fig. 7). Increase of the temperature resulted in an increase of the longest decay-component contribution. Such a finding is consistent with the multi-exponential decay being due to an intramolecular excimer. Increase of the temperature enabled molecular rotation (and thus, formation of the excimer) which competed with the deactivation from the $S_1$ resulting in higher percentage of the excimers.

**Table 3**
Decay times and the corresponding relative contributions obtained by SPT of **13** in $CH_3CN$ and in DMSO at different temperatures.

| Temperature/°C | $\tau_1$/ns (%) | $\tau_2$/ns (%) | $\tau_3$/ns (%) |
|---|---|---|---|
| 20[a] | 1.4 (22) | 6.4 (41) | 33 (36) |
| 20 | 0.8 (2) | 4.1 (93) | 60 (5) |
| 40 | 1.4 (7) | 4.0 (83) | 53 (9) |
| 80 | 0.4 (3) | 3.3 (72) | 36 (24) |

[a] Measured in $CH_3CN$.

To assign the decay components of **13** in $CH_3CN$ and DMSO, the SPT measurements were performed at wavelength region 390–520 nm, and time-resolved fluorescence spectra were constructed (see the Supporting Information). Long decay component in both solvents is clearly seen only at longer times after the laser pulse, indicating that it corresponds to aggregates (or excimers). Furthermore, the highest contribution of the decay component with 4.1 ns in DMSO, wherein fluorescence spectra do not indicate significant formation of aggregates, suggest that this decay component corresponds to the non-aggregated species. Consequently, decay component with ~4 ns seen in $CH_3CN$ and DMSO we tentatively assign to the non-aggregated molecules, whereas short (~1 ns) and long decay component we assign to aggregate or excimer.

All the above data indicate that **13** probably forms aggregates in both solvents. Most probably, in DMSO intramolecular excimers are formed by π,π-stacking of the pyrene chromophore in the $S_1$. On the other hand, in $CH_3CN$, molecules probably form both types of aggregates, intramolecular excimers due to the π,π-stacking in $S_1$, as well as intermolecular due to the H-bonds between the ureas and the π,π-stacking.

## 4. Conclusion

Adamantaneurea derivatives **1**–**13** were synthesized and their photophysical behavior investigated in two solvents with different H-bonding ability, $CH_3CN$ and DMSO. It was found that slight change in the structure of the molecule, e.g. introduction of the methylene spacer between the rigid adamantane part and the urea moiety, significantly changes photophysical properties. Molecules with the increased molecular flexibility such as **2** and **7** (compared to **1** and **6**, respectively) showed tendency to aggregate in

$CH_3CN$ solution resulting in fluorescence quenching. The aggregation is probably caused by intermolecular H-bonds between the urea moieties as well as due to the π,π-stacking. Contrary to naphthyl and 2-aminoanthryl derivative, pyrene **13** forms aggregates in both solvents which is in accordance with the increased possibility of π,π-stacking. From the anthracene derivatives, the highest tendency to aggregation was observed for 9-amino derivative **10** and 2-methyl derivatives **8** and **9**, whereas 9-methyl derivatives **11** and **12** probably do not form aggregates in DMSO solution in the investigated concentration range. Investigation of the photophysical behavior of **1**–**13** in these two solvent systems indicate that the best candidates for the development of anion sensor molecules are 2-naphthyl and 9-methylanthracene derivatives where formation of aggregates is minimal.

## Acknowledgements

This work was supported by the Croatian Ministry of Science, Education and Sports, Grant no. 098-0982933-2911, the Chinese "Program for New Century Excellent Talents in University" (NCET-09-0444), the "Fundamental Research Funds for the Central Universities" (lzujbky-2011-22) and (lzujbky-2012-k13), and the "International Cooperation Program of Gansu Province" (1104WCGA182). The support of The Croatian Ministry of Science, Education and Sports on the Chinese-Croatian bilateral project is also gratefully acknowledged. V. Blažek thanks J. Cui for the help with the SPT measurements. The authors thank Prof. C. Bohne, Prof. P. Wan, and the University of Victoria for the use of single photon timing set-up.

## Appendix A. Supplementary data

Supplementary data associated with this article can be found, in the online version, at doi:10.1016/j.jphotochem.2011.12.005.

## References

[1] J.-M. Lehn, Supramolecular Chemistry, VCH, Weinheim, 1995.
[2] (a) W. Deng, H. Yamaguchi, Y. Takashima, A. Harada, Angew. Chem. 119 (2007) 5236–5239;
W. Deng, H. Yamaguchi, Y. Takashima, A. Harada, Angew. Chem. Int. Ed. 46 (2007) 5144–5147;
(b) N. Sreenivasachary, J.-M. Lehn, Proc. Natl. Acad. Sci. U.S.A. 102 (2005) 5938–5943;
(c) M. Suzuki, M. Yumoto, M. Kimura, H. Shirai, K. Hanabusa, Chem. Eur. J. 9 (2003) 348–354;
(d) A. Ajayaghosh, V.K. Praveen, Acc. Chem. Res. 40 (2007) 644–656.
[3] (a) I. Aprahamian, T. Yasuda, T. Ikeda, S. Saha, W.R. Dichtel, K. Isoda, T. Kato, J.F. Stoddart, Angew. Chem 119 (2007) 4759–4763;
I. Aprahamian, T. Yasuda, T. Ikeda, S. Saha, W.R. Dichtel, K. Isoda, T. Kato, J.F. Stoddart, Angew. Chem. Int. Ed 46 (2007) 4675–4679;
(b) S. Sivakova, J. Wu, C.J. Campo, P.T. Mather, S.J. Rowan, Chem. Eur. J. 12 (2006) 446–456.
[4] (a) L. Hsu, G.L. Cvetanovich, S.I. Stupp, J. Am. Chem. Soc. 130 (2008) 3892–3899;
(b) V. Berl, M. Schmutz, M.J. Krische, R.G. Khoury, J.-M. Lehn, Chem. Eur. J. 8 (2002) 1227–1244.
[5] (a) T. Shimizu, M. Masuda, H. Minamikawa, Chem. Rev. 105 (2005) 1401–1444;
(b) P. Jonkheijm, A. Miura, M. Zdanowska, F.J.M. Hoeben, S. De Feyter, A. Schenning, F.C. De Schryver, E.W. Meijer, Angew. Chem. 116 (2004) 76–80;
P. Jonkheijm, A. Miura, M. Zdanowska, F.J.M. Hoeben, S. De Feyter, A. Schenning, F.C. De Schryver, E.W. Meijer, Angew. Chem. Int. Ed. 43 (2004) 74–78.
[6] (a) I. Yoshikawa, J. Sawayama, K. Araki, Angew. Chem. 120 (2008) 1054–1057;
I. Yoshikawa, J. Sawayama, K. Araki, Angew. Chem. Int. Ed. 47 (2008) 1038–1041;
(b) J.H. Ryu, H.J. Kim, Z.G. Huang, E. Lee, M. Lee, Angew. Chem. 118 (2006) 5430–5433;
J.H. Ryu, H.J. Kim, Z.G. Huang, E. Lee, M. Lee, Angew. Chem. Int. Ed. 45 (2006) 5304–5307;
(c) A. Ajayaghosh, R. Varghese, V.K. Praveen, S. Mahesh, Angew. Chem. 118 (2006) 3339–3342;
A. Ajayaghosh, R. Varghese, V.K. Praveen, S. Mahesh, Angew. Chem. Int. Ed. 45 (2006) 3261–3264;
(d) A. Ajayaghosh, R. Varghese, S. Mahesh, V.K. Praveen, Angew. Chem 118 (2006) 7893–7896;
A. Ajayaghosh, R. Varghese, S. Mahesh, V.K. Praveen, Angew. Chem. Int. Ed 45 (2006) 7729–7732.
[7] M. Kasha, H.R. Rawls, M.A. El-Bayoumi, Pure Appl. Chem. 11 (1965) 371–392.
[8] (a) E.E. Jelley, Nature 138 (1936) 1009–1010;
(b) G. Scheibe, Angew. Chem. 50 (1937) 212–219;
(c) T. Kobayashi (Ed.), J-aggregates, World Scientific Publishing Company, Singapore, 1996.
[9] (a) W.L. Lewschin, Z. Phys. 43 (1927) 230–253;
(b) E. Rabinowitch, L. Epstein, J. Am. Chem. Soc. 63 (1941) 69–78;
(b) T. Förster, E. König, Z. Elektrochem. 61 (1957) 344–348;
(c) K. Bergmann, C.T. O'Konski, Z. Phys. Chem. 67 (1963) 2169–2177;
(d) W. West, S. Pearce, J. Phys. Chem. 69 (1965) 1894–1903.
[10] (a) G. Scheibe, Z. Elektrochem. 52 (1948) 283–292;
(b) D. Möbius, Adv. Mater. 7 (1995) 437–444.
[11] (a) V. Czikklely, H.D. Försterling, H. Kuhn, Chem. Phys. Lett. 6 (1970) 207–210;
(b) J. Seibt, P. Marquetand, V. Engel, Z. Chen, V. Dehm, F. Würthner, J. Chem. Phys. 328 (2006) 354–362.
[12] (a) A. Bianchi, K. Bowman-James, E. Garcia-España (Eds.), Supramolecular Chemistry of Anions, VCH Verlag, Weinheim, 1997;
(b) J.L. Sessler, P.A. Gale, W.-S. Cho (Eds.), Anion Receptor Chemistry, RSC Publishing, Cambridge, 2006.
[13] (a) F.P. Schmidtchen, M. Berger, Chem. Rev. 97 (1997) 1609–1646;
(b) P.A. Gale, Coord. Chem. Rev. 213 (2001) 79–128;
(c) P.D. Beer, P.A.; Gale, Angew. Chem. Int. Ed. 40 (2001) 486–516;
(d) J.L. Sessler, J.M. Davis, Acc. Chem. Res. 34 (2001) 989–997;
(e) R.J. Fitzmaurice, G.M. Kyne, D. Douheret, J.D. Kilburn, J. Chem. Soc. Perkin Trans. 1 (2002) 841–864;
(f) P.A. Gale, Coord. Chem. Rev. 240 (2003) 191–221;
(g) R. Martínez-Máñez, F. Sancenón, Chem. Rev. 103 (2003) 4419–4476;
(h) P.A. Gale, Chem. Commun. (2005) 3761–3772;
(i) P.A. Gale, Coord. Chem. Rev. 250 (2006) 3219–3244;
(j) P.A. Gale, Acc. Chem. Res. 39 (2006) 465–475;
(k) V. Amendola, M. Bonizzoni, D. Estebán-Gómez, L. Fabbrizzi, M. Licchelli, F. Sancenón, A. Taglietti, Coord. Chem. Rev. 250 (2006) 1451–1470;
(l) C. Caltagirone, P.A. Gale, Chem Soc. Rev. 38 (2009) 520–563;
(m) P.A. Gale, Chem Soc. Rev. 39 (2010) 3746–3771;
(n) P.A. Gale, T. Gunnlaugsson, Chem. Soc. Rev. (2010) 3595–3596.
[14] (a) M. Renić, N. Basarić, K. Mlinarić-Majerski, Tetrahedron Lett. 48 (2007) 7873–7877;
(b) M. Alešković, I. Halasz, N. Basarić, M. Alešković, Tetrahedron 65 (2009) 2051–2058;
(c) M. Alešković, N. Basarić, K. Mlinarić-Majerski, K. Molčanov, B. Kojić-Prodić, M.K. Kesharwani, B. Ganguly, Tetrahedron 66 (2010) 1689–1698.
[15] V. Blažek, N. Basarić, K. Majerski, HR P20090186A.
[16] V. Blažek, N. Bregović, K. Mlinarić-Majerski, N. Basarić, Tetrahedron 67 (2011) 3846–3857.
[17] (a) C. Shi, Z. Huang, S. Kilic, J. Xu, R.M. Enick, E.J. Beckman, A.J. Carr, R.E. Melendez, A.D. Hamilton, Science 286 (1999) 1540–1543;
(b) L.A. Estroff, A.D. Hamilton, Angew. Chem. Int. Ed. 39 (2000) 3447–3450;
(c) S. Boileau, L. Bouteiller, F. Lauprêtre, F. Lortie, New J. Chem. 24 (2000) 845–848;
(d) F. Lortie, S. Boileau, L. Bouteiller, Chem. Eur. J. 9 (2003) 3008–3014;
(e) V. Simic, L. Bouteiller, M. Jalabert, J. Am. Chem. Soc. 125 (2003) 13148–13154;
(f) J. Courtois, I. Baroudi, N. Nouvel, E. Degrandi, S. Pensec, G. Docouret, C. Chenéac, L. Bouteiller, C. Creton, Adv. Funct. Mater. 20 (2010) 1803–1811.
[18] H.M. Keizer, J.J. González, M. Segura, P. Prados, R.P. Sijbesma, E.W. Meijer, J. de Mendoza, Chem. Eur. J. 11 (2005) 4602–4608.
[19] (a) S.S. Novikov, A.P. Hardin, L.N. Butenko, I.A. Novakov, S.S. Radchenko, Izv. Akad. Nauk. SSSR Ser. Khim. (1976) 2597–2599;
(b) H. Stetter, C. Wulff, Chem. Ber. 93 (1960) 1366–1371.
[20] M. Montalti, A. Credi, L. Prodi, M.T. Gandolfi, Handbook of Photochemistry, CRC Taylor and Francis, Boca Raton, 2006.
[21] I.B. Berlman, Handbook of Fluorescence Spectra of Aromatic Molecules, Academic Press, USA, 1971.
[22] S.R. Meech, D.V. O'Connor, D. Phillips, A.G. Lee, J. Chem. Soc., Faraday Trans. 2 (79) (1989) 1563–1584.
[23] (a) K. Suzuki, H. Tanabe, S. Tobita, H. Shizuka, J. Phys. Chem. A 101 (1997) 4496–4503;
(b) R. Montero, A. Longarte, Á. Peralta Conde, C. Redondo, F. Castaño, I. González-Ramírez, A. Giussani, L. Serrano-Anrés, M. Merchán, J. Phys. Chem. A 113 (2009) 13509–13518.
[24] (a) R. Custelclean, Chem. Commun. (2008) 295–307;
(b) J. Yang, M.B. Dewal, D. Sobransingh, M.D. Smith, Y. Xu, L.S. Shimizu, J. Org. Chem. 74 (2009) 102–110;
(c) S. Dawn, M.B. Dewal, D. Sobransing, M.C. Paderes, A.C. Wibowo, M.D. Smith, J.A. Krause, P.J. Pellechia, L.S. Shimizu, J. Am. Chem. Soc. 133 (2011) 7025–7032.
[25] M. Albrecht, C. Bohne, A. Granzhan, H. Ihmels, T.C.S. Pace, A. Schnurpfeil, M. Waidelich, C. Yihwa, J. Phys. Chem. A 111 (2007) 1036–1044.
[26] T. Förster, K. Kasper, Z. Electrochem. 59 (1956) 976–980.
[27] (a) R. Andriessen, N. Boens, M. Ameloot, F.C. De Schryver, J. Phys. Chem. 95 (1991) 2047–2058;
(b) K.A. Zachariasse, W. Kühnle, U. Leinhos, P. Reynders, G. Striker, J. Phys. Chem. 95 (1991) 5476–5488;
(c) K.A. Zachariasse, A.L. Macanita, W. Kühnle, J. Chem. Phys. B 103 (1999) 9356–9365.